THE JOURNAL OF PHYSICAL CHEMISTRY B

Article

pubs.acs.org/JPCB

Ultrafast Proton Shuttling in *Psammocora* Cyan Fluorescent Protein

John T. M. Kennis,*[,†] Ivo H. M. van Stokkum,[†] Dayna S. Peterson,[‡] Anjali Pandit,[†] and Rebekka M. Wachter*[,‡]

[†]Department of Physics and Astronomy and LaserLaB, Faculty of Sciences, Vrije Universiteit, De Boelelaan 1081, 1081 HV, Amsterdam, The Netherlands

[‡]Department of Chemistry and Biochemistry, Arizona State University, Tempe, Arizona 85287, United States

Supporting Information

ABSTRACT: Cyan, green, yellow, and red fluorescent proteins (FPs) homologous to green fluorescent protein (GFP) are used extensively as model systems to study fundamental processes in photobiology, such as the capture of light energy by protein-embedded chromophores, color tuning by the protein matrix, energy conversion by Förster resonance energy transfer (FRET), and excited-state proton transfer (ESPT) reactions. Recently, a novel cyan fluorescent protein (CFP) termed psamFP488 was isolated from the genus *Psammocora* of reef building corals. Within the cyan color class, psamFP488 is unusual because it exhibits a significantly extended Stokes shift. Here, we applied ultrafast transient absorption and pump−dump−probe spectroscopy to investigate the mechanistic basis of psamFP488 fluorescence, complemented with fluorescence quantum yield and dynamic light scattering measurements. Transient absorption spectroscopy indicated that, upon excitation at 410 nm, the stimulated cyan emission rises in 170 fs. With pump−dump−probe spectroscopy, we observe a very short-lived (110 fs) ground-state intermediate that we assign to the deprotonated, anionic chromophore. In addition, a minor fraction (14%) decays with 3.5 ps to the ground state. Structural analysis of homologous proteins indicates that Glu-167 is likely positioned in sufficiently close vicinity to the chromophore to act as a proton acceptor. Our findings support a model where unusually fast ESPT from the neutral chromophore to Glu-167 with a time constant of 170 fs and resulting emission from the anionic chromophore forms the basis of the large psamFP488 Stokes shift. When dumped to the ground state, the proton on neutral Glu is very rapidly shuttled back to the anionic chromophore in 110 fs. Proton shuttling in excited and ground states is a factor of 20−4000 faster than in GFP, which probably results from a favorable hydrogen-bonding geometry between the chromophore phenolic oxygen and the glutamate acceptor, possibly involving a short hydrogen bond. At any time in the reaction, the proton is localized on either the chromophore or Glu-167, which implies that most likely no low-barrier hydrogen bond exists between these molecular groups. This work supports the notion that proton transfer in biological systems, be it in an electronic excited or ground state, can be an intrinsically fast process that occurs on a 100 fs time scale. PsamFP488 represents an attractive model system that poses an ultrafast proton transfer regime in discrete steps. It constitutes a valuable model system in addition to wild type GFP, where proton transfer is relatively slow, and the S65T/H148D GFP mutant, where the effects of low-barrier hydrogen bonds dominate.

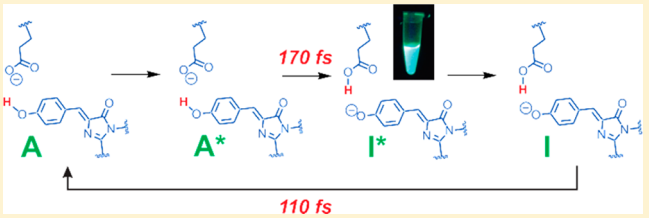

INTRODUCTION

Cyan fluorescent proteins (CFPs) derived from marine organisms of the class Anthozoa bear a chromophore chemically identical to that found in GFP. However, their emission spectra are blue-shifted from the default green state. Typically, members of the cyan color class exhibit absorption maxima from 430 to 460 nm and emission maxima from 474 to 496 nm.[1,2] Recently, a novel cyan fluorescent protein (CFP), termed psamFP488 in this work, was isolated from the genus *Psammocora* of reef building corals (order *Scleractinia*, family *Siderastreidae*).[1] Surprisingly, psamFP488 is one of only two proteins that were reported to display a substantially blue-shifted, broad absorption maximum around 404 nm, whereas the emission maximum was found to be within the range of colors reported for other CFPs.[1,2] Therefore, within its color class, psamFP488 appears to be one of only two CFPs known to exhibit a significantly extended Stokes shift. GFP-like proteins with similar excitation maxima include the highly engineered tagBFP (λ_{ex} = 402 nm) with blue emission at 457 nm and avGFP (*Aquorea victoria* GFP) with green emission at 508 nm.[3] CFPs with similar emission maxima include the engineered mTFP1 protein (λ_{em} = 492 nm), which has an absorption band centered on 462 nm. In addition, more blue-shifted CFPs have been developed that bear non-native chromophores derived from a tryptophan residue. These include the cerulean and turquoise line of variants,[4−6] highly

Special Issue: Rienk van Grondelle Festschrift

Received: January 31, 2013
Revised: March 26, 2013

   dx.doi.org/10.1021/jp401114e | *J. Phys. Chem. B* XXXX, XXX, XXX−XXX

engineered proteins that absorb at ~433 nm and emit at ~475 nm.

CFPs with a large Stokes shift may prove useful in some types of live-cell imaging applications, such as dual color monitoring by excitation of two different FPs at the same wavelength.[7] In particular, an extended Stokes shift may be beneficial in FRET experiments frequently used to monitor macromolecular proximity on a subcellular level. To date, the most common FP pairs used in FRET experiments involve CFPs and yellow fluorescent proteins (YFPs). PsamFP488 may prove advantageous as a donor fluorophore in combination with acceptors such as Venus or mOrange,[8] as cross-excitation would be minimized due to the large separation of excitation and emission wavelengths. Notably, the sensitivity of multiparameter live cell imaging involving two FRET pairs with fine-tuned optical properties could be enhanced by the high quantum yield of psamFP488 when using an excitation wavelength provided by a 405 nm laser line.[9]

GFP and many of its variants exhibit large Stokes shifts that find their origin in an ESPT process that results in deprotonation of the chromophore and subsequent fluorescence emission from the anionic chromophore.[3,10−14] Recently, ESPT appears to be a frequently occurring feature in photoreceptor proteins,[15−18] sometimes coupled to electron transfer.[19−26] With its simple light-driven proton transfer reaction along a chain of a water molecule and two amino acids, GFP can be regarded as an attractive and compact model system to understand the basic principles of proton transfer in biological systems. ESPT in GFP has been well characterized by means of time-resolved spectroscopy and X-ray crystallography,[10−12,14,27−32] and a proton transfer wire was identified that involved a hydrogen-bond network of the chromophore, bound water, a serine side chain and a terminal proton acceptor, Glu-222.[10,14,29,32] In particular, upon near-UV excitation of the neutral, protonated chromophore, the (stimulated) emission of the deprotonated chromophore was found to rise biphasically with time constants of 3 and 15 ps, corresponding to the ESPT process.[10−12,28,29] Ultrafast mid-IR spectroscopy demonstrated that, concomitant with the rise of anionic chromophore emission, Glu-222 became protonated.[27,30] On the basis of photoselection ultrafast mid-IR experiments on wild type and mutant GFP, it was proposed that the biphasic proton transfer kinetics found their origin in two distinct conformers of Glu-222.[30] Recent work showed that the biphasic proton transfer kinetics may be related to a distinct excited-state intermediate state involving an evolved low-barrier hydrogen bond (LBHB) between chromophore and structural water, resulting in dual emission, along with significantly correlated proton motion along the three-hydrogen-bond proton wire.[31]

On the basis of X-ray structures of homologous fluorescent proteins, one can conclude that a GFP-like proton wire is lacking in psamFP488. This raises the question as to what mechanism underlies its large Stokes shift. Here, we applied ultrafast transient absorption and pump−dump−probe spectroscopy to investigate the mechanistic basis of psamFP488 fluorescence, complemented by homology modeling, fluorescence quantum yield, and dynamic light scattering measurements.

MATERIALS AND METHODS

Cloning, Expression, and Purification of psamFP488. The gene coding for full-length psamFP488 was PCR-amplified from a pGEM-T expression plasmid. PCR amplification, directional cloning of the PCR product into a linear pET151/DTOPO vector (Invitrogen), and transformation into *Escherichia coli* BL21(DE3) competent cells (Invitrogen) were carried out according to the manufacturer's instructions. Plasmid was prepared from individual transformant colonies using the QIAprep kit (Qiagen). Single colonies were cultured overnight at 37 °C in 25 mL of Luria−Bertani (LB) media with 100 mg/L carbenicillin, used to inoculate 1 L of LB/carbenicillin, and cultured at 37 °C until the OD600 reached 0.8. The cultures were cooled to 25 °C. Protein expression was induced by the addition of 1 mM IPTG and allowed to proceed for 4 h at 25 °C. Cells were harvested by centrifugation and frozen at −80 °C.

Cell paste was suspended in 50 mL of 25 mM HEPES pH 7.9, 300 mM NaCl, 10% glycerol, 3 mM BME, and 0.1 mM PMSF and then disrupted by sonication. The lysate was centrifuged, and the supernatant was passed through a 0.2 μm syringe filter before loading onto a nickel-nitrilotriacetic acid Superflow column (Qiagen). N-Terminally 6His-tagged protein was purified using an imidazole step gradient in 50 mM HEPES, pH 7.9, 300 mM NaCl. Fractions containing the His-tagged protein were pooled, 1.2 mg of tobacco etch virus (TEV) protease was added, and the sample was dialyzed overnight at 4 °C against 1 L of 50 mM Hepes pH 7.9, 300 mM NaCl. The dialysate was reapplied to a nickel-nitrilotriacetic acid column, and purified psamFP488 was collected in the early fractions. Protein was concentrated and buffer-exchanged into 50 mM HEPES pH 7.0, 300 mM NaCl. Aliquots of purified protein were flash frozen in liquid nitrogen and stored at −80 °C in buffer containing 50 mM HEPES pH 7.9 and 300 mM NaCl. Protein concentration was determined by absorbance at 280 nm using a theoretical extinction coefficient equal to ε = 22 920 M^{-1} cm^{-1}. Steady-state absorbance and fluorescence spectra were collected on psamFP488 in 50 mM HEPES pH 7.9, 300 mM NaCl, using a Shimadzu UV-2401 spectrophotometer and a Jobin Yvon Fluoromax-3 fluorimeter. Fluorescence scans were collected at 1.0 nm increments utilizing an integration time of 1.0 s and a slit width of 1.0 nm for both excitation and emission. For the ultrafast spectroscopic experiments, the absorbance of the psamFP488 samples was adjusted to 0.3−0.4 per mm at pH/pD 7.9.

Determination of the Quantum Yield of Fluorescence. The fluorescence quantum yield of psamFP488 (0.16 mg/mL) was determined using fluorescein as a standard (1 μM in 0.1 M NaOH) according to published procedures.[33] Fluorescence emission intensity was integrated upon excitation at 465 and 417 nm. The buffer for all protein preparations was 20 mM HEPES pH 7.9, 20 mM NaCl. The data were fit to the following equation: $\Phi = \Phi_R[I/I_R]\,[OD_R/OD]$, where Φ is the quantum yield, I is the integrated intensity, and OD is the optical density at 465 nm or 417 nm. R refers to the reference fluorophore with quantum yield 0.95.

Dynamic Light Scattering. Dynamic light scattering experiments were performed using a DynaPro NanoStar instrument (Wyatt Technology Corp., Santa Barbara, CA,) and analyzed using the software Dynamics 7.0.3.12 (Wyatt Technology Corp.). Briefly, 80 μL aliquots of 0.5−5.0 mg/mL psamFP488 in 20 mM HEPES pH 7.9, 137 mM NaCl, were spin filtered for 3 min at 3000*g*, using 0.1 μm spin filters (Millipore). Filtrates were transferred to disposable UVette cuvettes (Eppendorf, Hauppauge, NY) for data collection at 20 °C. Scattered light intensity fluctuations were averaged from 40

dx.doi.org/10.1021/jp401114e | J. Phys. Chem. B XXXX, XXX, XXX−XXX

acquisitions (5 s each), and the resulting autocorrelation functions fit via the regularization method. The hydrodynamic radius was estimated assuming a spherical particle shape.

Spectroscopy. The time-resolved studies were performed on a laboratory-built femtosecond transient absorption setup.[19,34,35] The system was pumped by a pulsed amplified femtosecond Ti:sapphire laser system (Legend or Libra USP seeded by a Vitesse 800-2, Coherent, Mountain View) with an average output of 3.7 W from 1 kHz, 45 fs pulses, centered at 800 nm. 1 W of the output was used for pumping an optical parametric amplifier (OPA, OperA Solo, Coherent) for creating tunable pump pulses; a small fraction was used for preparation of the probe pulse by supercontinuum generation in a rotating 2 mm CaF_2 plate. For the transient absorption experiments, an excitation pulse at 410 nm was prepared by second harmonic generation in a BBO crystal out of 820 nm pulses generated in the OPA. The pump energy was adjusted to 60 nJ with a spot size of 200 μm. For the pump−dump−probe experiments, the output of the amplifier was split in three paths. The first path was frequency doubled in a BBO crystal to give the 400 nm pump pulses. The second path was used to pump an OPA, producing dump pulses at 510 nm, and the third path was focused into a rotating CaF_2 plate, generating broadband probe pulses. Pump pulses were modulated with a chopper at 500 Hz, and the dump pulses at 250 Hz. Both were delayed via 60 cm translation stages. This generated four data sets: pump−dump−probe, pump−probe, dump−probe, and control (neither pump nor dump). Pump and dump pulses were set at magic angle relative to the probe pulse and parallel to each other. The pump pulse energy was set at 110 nJ, and the dump pulse energy, at 100 nJ. In the spectrograph (Oriel MS127i) 1/8m, a 300 grooves/mm 500 nm blazed grating was used. Detection was based on a PIN diode array (256 pixels) run by laboratory-built electronics and software including single shot statistics and noise discrimination. The signal was recorded in one 300 nm wide spectral window. The sample was placed in a 1 mm path length fused silica cuvette held by a shaker. The buffer for all protein preparations was 20 mM HEPES pH/pD 7.9, 20 mM NaCl. For the H_2O/D_2O buffer exchange experiments, equal sample aliquots were dissolved in H_2O or D_2O buffer and left to equilibrate overnight prior to the experiment.

Data Analysis. The data were fitted by using global and target analysis,[12] with the extension for pump−dump−probe data described in refs 12 and 36.

RESULTS

Absorption and Fluorescence Spectra, Quantum Yield, and Quaternary Structure. Figure 1 shows the fluorescence excitation and fluorescence spectra of psamFP488. The absorption spectrum (not shown) was essentially identical to the fluorescence excitation spectrum. The absorption spectrum shows a main band with a maximum at 407 nm and a shoulder at 460 nm, and agrees with that published earlier.[1] The psamFP488 chromophore does not appear to titrate with pH, as the absorbance spectra remain unmodified between pH 4 and 10. The fluorescence has a single broad band with a flat maximum from 485 to 490 nm, corresponding to a Stokes shift of 4500 cm^{-1}, and is slightly blue-shifted from that published earlier.[1] As compared to GFP,[3] the absorption and fluorescence bands are broader and less resolved. In particular, the fluorescence spectrum has a width of 60 nm (2500 cm^{-1}), compared to 30 nm (1000 cm^{-1}) for GFP. The quantum yield of psamFP488 fluorescence measured on three independently

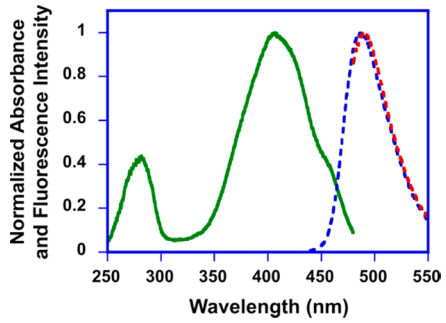

Figure 1. Normalized fluorescence and fluorescence excitation spectra of psamFP488. For the excitation scan (green solid line), the emission was monitored at 488 nm. For the emission scans (dotted lines), the excitation wavelength was set to 415 nm (blue) or 460 nm (red).

prepared protein preparations was determined to be 0.850 ± 0.038 (n = 3) with 465 nm excitation and 0.876 ± 0.007 (n = 2) with 417 nm excitation, slightly lower than the published value of 0.96.[1]

On the basis of DLS measurements, the quaternary structure of psamFP488 was determined to be a homotetramer, as supported by sequence homology to other *Anthozoa* FPs known to be tetrameric.[37] DLS spectra collected at 20 °C on samples containing 0.5−5.0 mg/mL protein appeared monodisperse, and the calculated hydrodynamic radius was consistent with 4.1 ± 0.2 (n = 5) protein chains per particle.

Characterization of the Chromophore Environment Based on Close Homologues. In spite of extensive efforts, to date, diffraction-quality crystals of psamFP488 have not been obtained yet. A standard BLAST protein database search indicates that the closest sequence homologue to psamFP488 is a CFP derived from *Montipora efflorescens* (71% sequence identity); however, a three-dimensional structure is not available for this protein. A structural database search indicates that seven high-resolution X-ray structures are available for FPs exhibiting 59−61% sequence identity to psamFP488. All of these proteins were originally isolated from the button polyp *Zoanthus sp.*, including the yellow fluorescent protein zFP538 (61% identity),[37] the red fluorescent zRFP574, and the green fluorescent zGFP506.[38] Previous works have demonstrated that the chromophore environment of many naturally occurring CFPs, such as amFP486 and dsFP483, closely resembles that of the yellow and red fluorescent proteins zFP538 and DsRed, and their immediate homologues.[33,39] Therefore, we expect that psamFP488 bears the typical GFP-like two-ring chromophore consisting of the benzylidene imidazolinone group derived from a QYG tripeptide sequence (residues 66−68). Due to the high quantum yield for fluorescence, the chromophore π-system is likely held in a rigidly planar conformation by the surrounding protein matrix. On the basis of the high level of conservation of buried residues, the structural features of the chromophore environment are expected to be similar to zFP538 (Figure 2). When comparing residue positions immediately surrounding the chromophore, zFP538 and psamFP488 contain identical residues with the sole exception of position 167 (residue numbering according to avGFP), where zFP538 bears a methionine (Met-167) and psamFP488 a glutamic acid (Glu-165 according to psamFP488 residue numbering). Following convention, avGFP residue numbering will be used throughout the text. A structural model of psamFP488 was generated by introducing the in silico mutation M167E, followed by selection of a common glutamic acid side chain rotamer with miminal

dx.doi.org/10.1021/jp401114e | J. Phys. Chem. B XXXX, XXX, XXX−XXX

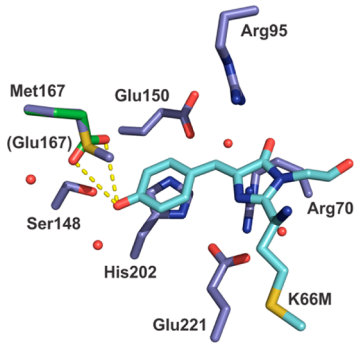

Figure 2. Active site structure of the psamFP488 homologue zFP538-K66 M (pdb code 1XA9)[37] bearing the standard green-fluorescent chromophore found in GFP (blue and cyan). In psamFP488, the position equivalent to Met167 is occupied by a glutamic acid (green), computer-modeled in a rotamer conformation that provides minimal steric clash. Suggested hydrogen bonding interactions with the chromophore are indicated as dashed yellow lines (3.3 and 3.4 Å in the model). Arg95, Glu150, Ser148, His202, Glu221, and Arg70 are conserved in psamFP488. Residue 66 is occupied by Gln in psamFP488 (not shown).

steric interference (Figure 2). The model suggests that the two Glu-167 carboxy oxygen atoms are positioned within hydrogen bonding distance to the chromophore's phenolic hydroxyl group (3.3 and 3.4 Å without energy minimization). This scenario would provide a hydrogen bonded pathway for rapid proton transfer to Glu-167 upon chromophore excitation.

In dsFP483, a hydrogen-bonded network leading from Ser-148 to Glu-150 has been identified, and involves two crystallographically ordered water molecules.[33] A similar network involving Glu-167 and Glu-150 could also exist in psamFP488 (Figure 2), suggesting that, at least in principle, either Glu-167 or Glu-150 could serve as a proton sink for ESPT.

It has been noted previously that the replacement of a positively charged residue with a polar one in position 167 may be coupled to cyan light emission in a DsRed-like protein environment.[33] This idea seems to hold true for psamFP488 as well, as Glu-167 may become protonated neutral upon ESPT, thus providing a similar electrostatic environment as a histidine residue in dsFP483 or a solvent molecule in amFP486.[39] In support of this notion, position 167 was identified previously as an important determinant of cyan color based on statistical sequence analysis.[40]

Ser-148 is conserved among many Anthozoa FPs, including dsFP483, amFP486, zFP538, and DsRed (Figure 2).[33] In addition, the quadrupole arrangement of charges consisting of Glu-150, Arg-70, His-202, and Glu-221 is highly conserved among many coral FPs including amFP486, zFP538, and psamFP488. However, not all cyan proteins bear this particular charge network, as dsFP483 contains a threonine residue in position 202.[33]

Photoconversion. PsamFP488 undergoes photoconversion upon near-UV illumination. Figure S4 (Supporting Information) shows the absorption spectrum before and after near-UV laser illumination. We observe that the 407 nm band has decreased, while the 460 nm shoulder has increased. This phenomenom is similar to that observed in GFP, where the A band photoconverts to the B band under near-UV illumination, corresponding to deprotonation of the chromophore and decarboxylation of the terminal Glu proton acceptor.[41] The observation of a similar process in psamFP488 supports the idea that the 407 nm band corresponds to a protonated chromophore, and the 460 nm shoulder to a deprotonated chromophore. Photoconversion puts limits on the data acquisition with ultrafast spectroscopy; the data shown in Figures 3 and 4 were taken on samples that had undergone less than 10% conversion.

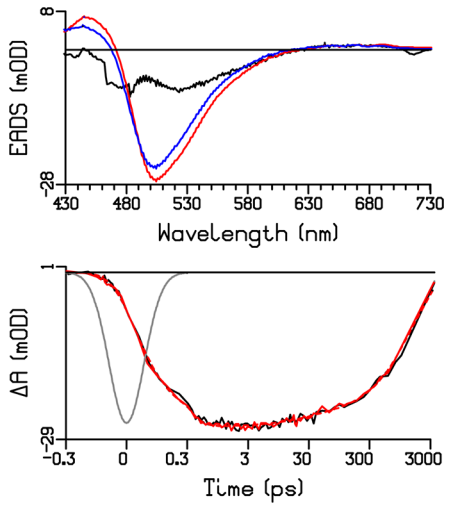

Figure 3. Transient absorption spectroscopy on psam488. (upper panel) Evolution-associated difference spectra (EADS): black, 170 fs; red, 42 ps; blue, 1.6 ns. (lower panel) Kinetics in H_2O (black) and D_2O (red) at 500 nm. IRF is depicted in gray. The time axis is linear from −0.3 until 0.3 ps relative to the location of the IRF and logarithmic thereafter.

Ultrafast Transient Absorption Spectroscopy. To investigate the origin of the large Stokes shift in psamFP488, we performed ultrafast transient absorption spectroscopy. The sample was excited at 410 nm, and the resulting absorbance changes were recorded in a spectral region between 430 and 730 nm. The time-resolved data were globally analyzed using a sequential model with increasing lifetimes (1 → 2 → 3 → 4...).[12] The corresponding evolution-associated difference spectra (EADS) are displayed in Figure 3 (upper panel). Three components were required for an adequate fit of the data, with lifetimes of 170 fs, 24 ps, and 1.6 ns. In addition, a pulse follower was included in the analysis to account for coherent and cross-phase modulation artifacts, and for stimulated Raman scattering from the aqueous buffer. The first EADS (black line) has a lifetime of 170 fs and shows an overall low signal, with main negative amplitude from 470 to 520 nm, corresponding to stimulated emission. The second EADS (red line) rises in 170 fs and has a lifetime of 25 ps. It is characterized by a pronounced stimulated emission band at 510 nm and excited-state absorption between 420 and 470 nm. Its amplitude is 3 times larger than the first EADS, which implies that the stimulated emission band at 510 nm is not formed instantaneously but rises primarily with a time constant of 170 fs. This time constant is close to the instrument response function (IRF) (204 fs fwhm) but can be well estimated because the time position and width of the IRF can be very accurately estimated through the stimulated Raman scattering signal from the aqueous buffer which arises near 475 nm, close to the maximum of the stimulated emission. The second EADS represents the difference spectrum of the Stokes-shifted

dx.doi.org/10.1021/jp401114e | J. Phys. Chem. B XXXX, XXX, XXX−XXX

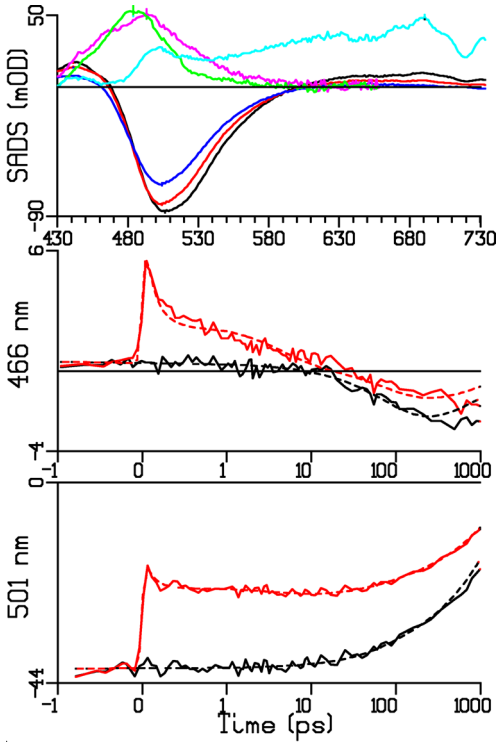

Figure 4. Pump–dump–probe results on psam488. (upper panel) Species-associated difference spectra (SADS) estimated from target analysis. Key: black, 3.5 ps; red, 81 ps; blue, 1.4 ns; all three excited-state intermediates, two GSIs, lifetimes 0.11 ps (86%, green) and 3.6 ps (14%, magenta), and cyan solvated electron (8 ns). Vertical bars at extrema indicate estimated standard errors. (middle and lower panels) Kinetics at selected wavelengths (indicated as ordinate labels). Key: black pump–probe, red pump–dump–probe, dashed lines indicate fits. Time axis is linear from −1 until 1 ps relative to the location of the dump IRF maximum and logarithmic thereafter.

emitting state of psamFP488, and involves a broad stimulated emission band that peaks near 500 nm, and excited-state absorption near 450 nm. The second EADS then evolves in the third EADS (blue line) in 25 ps, which represents only a very minor spectral evolution with a slight blue-shift and amplitude decrease of the difference spectrum. This spectral evolution may correspond to slow solvation effects of the excited chromophore in the protein matrix, and/or to minor singlet–singlet annihilation that possibly arises from multiple excitations on the same tetrameric complex. The third EADS finally relaxes to the psamFP488 ground state with a fluorescence lifetime of 1.6 ns.

Figure 3 (lower panel) shows a kinetic trace at 500 nm (black line), where stimulated emission is probed. In line with the results from the global analysis procedure, the rise of stimulated emission is very rapid, after which it decays to zero almost monoexponentially.

In GFP, the large Stokes shift between the A band and the fluorescence at 509 nm is caused by an ESPT process whereby the neutral chromophore deprotonates on a ps time scale. This ESPT process is subject to a significant KIE of about 3.[10,12] We performed the same transient absorption experiments on psamFP488 in D_2O buffer to check for a KIE in the rise of the stimulated emission, shown in Figure 3 (lower panel) as the red line. We observed that the kinetics in H_2O and D_2O buffer were indistinguishable, implying that, in contrast to the situation in GFP, there is no KIE associated with the dynamic Stokes shift in psamFP488.

Pump–Dump–Probe Experiments. Pump–dump–probe spectroscopy is a powerful variant of transient absorption spectroscopy where a second actinic pulse is applied at a certain delay after the pump pulse in order to move the population from the excited-state to the ground-state potential energy surface. It has been applied to many photobiological systems[42−48] and mimics,[49] and has given unprecendented insights into reaction connectivity, ground-state dynamics, and hidden reaction intermediates.

In GFP, the ground state of the deprotonated chromophore, referred to as I, was observed directly with pump–dump–probe spectroscopy.[12,31,32,36] With this technique, the anionic chromophore excited state I* is "dumped" to the ground state using a "dump" pulse that is resonant with the stimulated emission. In GFP, a clear anionic ground-state absorbance I was observed similar to that of mutants with mutagenically stabilized I states, and became reprotonated in 400 ps. Thus, pump–dump–probe spectroscopy is a powerful tool to assess light-driven proton transfer reactions in fluorescent proteins.

To investigate whether ESPT occurs in psamFP488 upon near-UV excitation, we performed a pump–dump–probe experiment with excitation at 400 nm and dump at 510 nm that was applied 10 ps after the initial excitation pulse. Figure 4 shows kinetic traces of pump–probe (black line) and pump–dump–probe (red line) experiments with detection at 501 nm (Figure 4, lower panel) and 466 nm (Figure 4, middle panel). At 501 nm, we observe that, after the dump pulse, 36% of the stimulated emission disappears, indicating that we were successful in dumping the psamFP488 excited state to the ground state. At 466 nm, we observe that an initially nearly zero signal becomes positive upon application of the dump pulse, indicating that a species absorbing at that wavelength is formed by the dump pulse. This positive absorption feature disappears on two time scales: 0.11 ps (86%) and 3.6 ps (14%). Subsequently, the pump–dump–probe signal further evolves temporally identically to the pump–probe signal but at diminished amplitude. These observations indicate that, indeed, a transient ground-state product is formed that absorbs at a wavelength expected for a deprotonated chromophore.

We performed a simultaneous target analysis of pump–probe and pump–dump–probe data to extract the spectral signatures and kinetics of the states involved,[12,31,36] in particular of the short-lived ground-state intermediates that were produced by the dump pulse. Fits at all wavelengths between 441 and 535 nm are depicted in Figures S1 and S2 (Supporting Information), demonstrating the excellent quality of the fit, and in particular the disappearance on two time scales: 0.11 ps (86%) and 3.6 ps (14%). At wavelengths around 466 nm, the fit deviates somewhat from the data at long time delays. The absolute magnitude of the signals is very small in this wavelength region and it concerns only a few time points, so their deviation from the fit contributes little to the overall fit quality. In principle, the pump–probe data (which is simultaneously obtained with the pump–dump–probe data) should be identical to that presented in Figure 3. However, we found some differences in the spectral evolution that result from the higher pump pulse energy that was required to create sufficient excited-state population to perform a pump–dump–probe experiment:

dx.doi.org/10.1021/jp401114e | J. Phys. Chem. B XXXX, XXX, XXX–XXX

(i) The sub-ps time scales around zero pump delay could not be reliably modeled due to a strong coherent/cross phase modulation artifact around time zero. To formally fit the data on the sub-ps time scale, a 680 fs component was included and left without interpretation.

(ii) A signature from photoionization was apparent in the pump−probe and pump−dump−probe. Photoionization upon femtosecond near-UV excitation was demonstrated before in the GFP chromophore,[50] PYP,[44] and BLUF domains[51] and results from a resonantly enhanced two-photon excitation process, leading to electron ejection from the chromophore and formation of a solvated electron. Its spectral signature is a broad, featureless absorption that extends toward the near-IR. In addition, the corresponding GFP chromophore cation radical absorbs around 450 nm.[50] The photoionization process was taken into account by a separate component formed instantly by the pump pulse that had a lifetime of 8 ns. The magnitude of the cyan SADS (relative to the other SADS) depends upon the amount of photoionization. Here we arbitrarily put this at 20%, to demonstrate its shape.

(iii) A minor 3.5 ps relaxation process (from the black to the red SADS) was observed in this pump−probe data set, which may partly correspond to geminate recombination of the solvated electron.[52] We could not separate this contribution from the true psamFP488 spectral evolution, and therefore left it in the target analysis without further interpretation.

The kinetic model included a sequential model for the evolution of the pump−probe signal with four time constants, a parallel instantaneous component to account for the solvated electron, and a pulse follower to account for coherent and cross phase modulation artifacts around pump time zero. For the pump−dump−probe signals, a population decrease due to the dump pulse at 10 ps was included, a transient ground-state intermediate product formed by the dump pulse, and a pulse follower to account for coherent and cross phase modulation artifacts at the time (10 ps) of the dump pulse in the spectral range between 498 and 518 nm.

Figure 4 (upper panel) shows the species-associated difference spectra (SADS), and the accompanying concentration profiles are depicted in Figure S3 (Supporting Information). The analysis shows that 37% of the psamFP488 excited states is dumped at 10 ps. The ground-state intermediate species produced by the dump pulse are denoted by the light green and magenta SADS. They have an overall positive amplitude, which supports the notion that they are true ground-state molecular species. The absorption maximum of the dominant SADS (light green, 86% of the amplitude decay) is located at 484 nm, consistent with a deprotonated chromophore. Its lifetime of 110 fs indicates that it is extremely short-lived. The minor GSI component (magenta, 14% of amplitude decay) has a lifetime of 3.5 ps and has an absorption maximum around 498 nm.

The sequential evolution of the psamFP488 excited state is shown as black (3.5 ps) → red (81 ps) → blue (1.4 ns). The photoionization SADS is shown in cyan and shows the typical broad and featureless solvated electron absorption, along with a bleach signal superimposed at 470 nm.

DISCUSSION

Ultrafast Proton Transfer in psamFP488 Electronic Ground and Excited States. For the sake of reasoning, we will first discuss the results from the pump−dump−probe experiments. We observe that the 510 nm dump pulse produces a ground-state species that has a maximum absorption at 484 nm and a remarkably short lifetime of 110 fs. We will refer to this species as I. I has an overall broad absorption with no resolved vibronic structure and a width of 1800 cm^{-1}, which is similar to that of the psamFP488 fluorescence (2500 cm^{-1}, Figure 1). We therefore assign I to an anionic ground-state chromophore that is formed upon dumping of the anionic excited-state chromophore, similar to previous experiments on GFP.[12]

The small Stokes shift of the psamFP488 fluorescence with respect to I is slightly smaller than that found for the dumped I ground state of GFP[12] and is consistent with other GFP-like proteins with anionic chromophores, which is often ∼5 nm.[3] The large spectral width of absorption and emission spectra, in combination with an apparent absence of vibronic structure, is observed in all psamFP488 spectra: steady-state absorption, fluorescence, transient absorption spectra and I, and is probably related to extensive inhomogeneous broadening and/or structural heterogeneity. In addition, I has an absorption tail to red that is unmistakenly present in the data. It probably means that I is dumped on a distorted, broad region of the ground-state potential energy surface.

The pump−dump−probe experiment demonstrates that (i) emission takes place from an anionic chromophore and (ii) that the chromophore was not anionic prior to excitation; otherwise, the I species would not be observed (dumping would then result in zero absorbance change). We hence conclude that the near-UV absorption band of psamFP488 corresponds to a neutral, protonated chromophore and that ESPT takes place upon near-UV excitation. Given the transient absorption experiments in Figure 3, we conclude that the rapid rise of stimulated emission in 170 fs represents the ESPT process that results in an anionic excited-state chromophore. Upon dumping of the excited state, I is formed and disappears in 110 fs, meaning that the proton is shuttled back to the chromophore with that time constant.

We may thus summarize the psamFP488 proton transfer cycle as depicted in Figure 5. In analogy with GFP, near-UV excitation of the A band results in an A*-like excited state. In 170 fs, ESPT takes place to result in an I*-like deprotonated excited state. The speed of this reaction implies that this is a barrierless reaction. Dumping of the excited state produces the ground-state anionic chromophore I, which is rapidly reprotonated in 110 fs to reform the neutral ground state A. A small fraction of dumped ground states (14%) is reprotonated in 3.5 ps. These are striking results that indicate that proton transfer in biological hydrogen-bonded systems may intrinsically occur on a 100 fs time scale. To the best of our knowledge, this novel result represents the fastest experimentally observed proton transfer process in a molecular ground state. The observed phenomena are similar to those of GFP[12] but 20 times faster in the excited state and nearly 4000 times faster in the ground state: in GFP, ESPT occurs biphasically in 3−15 ps,[10−12] while, in the ground state, the proton is shuttled back in 400 ps.

While we assigned the spectral evolution of psamFP488 in terms of proton transfer processes, we did not observe a H/D

dx.doi.org/10.1021/jp401114e | J. Phys. Chem. B XXXX, XXX, XXX−XXX

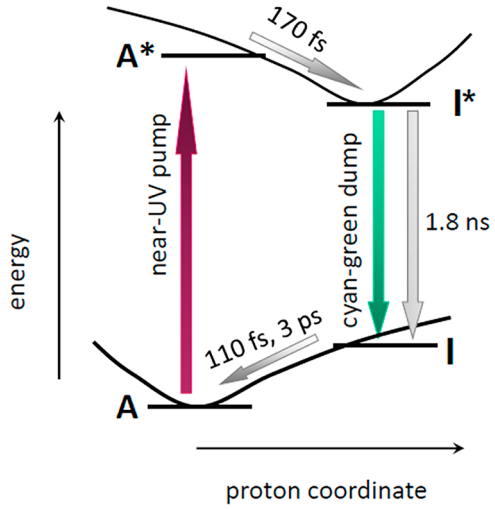

Figure 5. Schematic model for psamFP488 proton transfer processes induced by pump and dump pulses. See text for details.

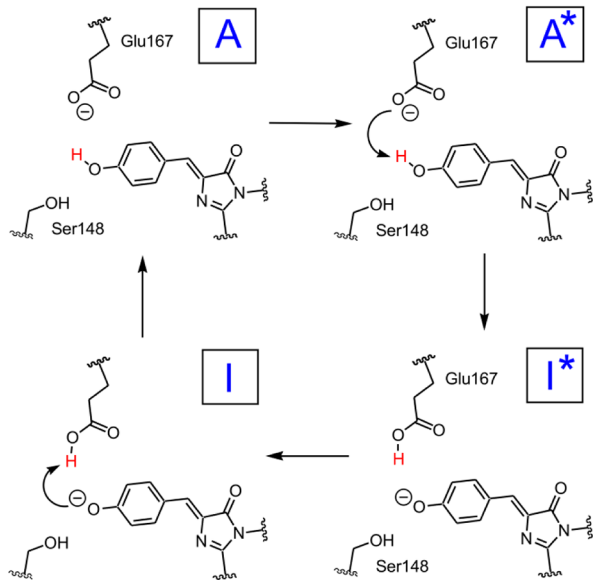

Figure 6. Proton shuttling scheme of psamFP488. The A → A* and I* → I transitions are driven by pump and dump pulses, respectively. The A* → I* transition occurs through ESPT in 170 fs, while the I → A transition occurs through proton transfer in the ground state in 110 fs. See text for details.

kinetic isotope effect on the 170 fs ESPT process. In contrast, GFP exhibits strong kinetic isotope effects of 3 for the ESPT reaction[10] and 8 for the ground-state proton back-shuttle.[12] It is important to note here that proton transfer processes do not necessarily exhibit kinetic isotope effects, and isotope effects may vanish in the fully adiabatic limit,[53] which may apply to strongly hydrogen-bonded systems. We did not test for H/D kinetic isotope effects in the pump−dump−probe experiment due to sample quantity limitations.

Origin of Ultrafast Proton Transfer Processes. The question arises what the origin is of the exceedingly fast ESPT reaction of 170 fs as observed in psamFP488. In the absence of a high-resolution X-ray structure and detailed information on the hydrogen-bond pattern around the chromophore, we can only speculate on this issue. It should first be noted that ESPT can be an intrinsically fast process in case the donor and acceptor are positioned in a favorable geometry.[54] ESPT in GFP is significantly slower (3−15 ps) than this limiting case. It was proposed that slow skeletal chromophore motions are required to bring the chromophore in optimal geometry for ESPT, and hence are rate-limiting to the process.[55] In addition, it was recently found that ESPT in GFP may be more complex than previously thought, with key roles of evolving short hydrogen bonds and low-barrier hydrogen bonds between chromophore and structural water, and significant correlated proton motion along the three-hydrogen-bond proton wire.[31] In psamFP488, the proton "wire" may involve only one hydrogen bond, between the chromophore and putative proton acceptor Glu-167. In contrast to the situation in GFP, chromophore and Glu-167 may be positioned in a favorable hydrogen-bonding geometry for prompt proton transfer without the need for prior structural evolution. The negative charge on Glu may result in a short, strong hydrogen bond, which may contribute to the observed fast ESPT. Figure 6, right, schematically depicts the ESPT process between the chromophore and Glu-167.

A remarkable observation in this work is that, upon dumping of the excited state, the proton is shuttled back to the anionic chromophore in the molecular ground state with a time constant of 110 fs, which is even faster than the rapid forward ESPT. This observation indicates that the ground-state proton transfer reaction proceeds barrierless, as much as it does in the excited state. It is likely that the favorable hydrogen-bonding geometry that preexisted for ESPT is maintained after dumping the excited state, and that the proton is not transferred further than the putative proton acceptor Glu-167. Hence, in contrast to GFP, the proton is not transferred over a proton wire but can reprotonate the chromophore immediately after the pK_a of the latter is switched by the dump pulse. Figure 6, left, schematically depicts the reverse proton transfer process between the chromophore and Glu-167 in the ground state.

We observed a minor slow reprotonation phase of 3.5 ps in the pump−dump−probe experiment (green SADS in Figure 4, 14% amplitude). The SADS is slightly red-shifted and broadened with respect to that of the major 110 decay phase. It likely represents a specific hydrogen-bond conformation of the dumped ground state I that is relatively unfavorable for proton transfer; note that this phase still is 100 times faster than that observed in GFP.[12] A more remote sink such as Glu150 could provide the basis for the observed slow component of ground-state reprotonation, whereas an adjacent sink such as Glu-167 could provide the basis for the observed ultrafast component of the chromophore reprotonation process (110 fs).

Comparison with the S65T/H148D GFP Mutant. A sub-ps ESPT reaction (estimated at <300 fs) was recently proposed but not directly observed for the photoactivated pB state of a PYP mutant.[17] In BLUF domains, a rapid, <1 ps proton transfer process was observed in concert with electron transfer.[51] It is interesting to compare the dynamics as observed here with those reported on the S65T/H148D mutant of GFP. In that mutant, the proton transfer pathway was "rewired": instead of forming a proton wire of chromophore, bound water, Ser-205, and Glu-222, the X-ray structure showed that the proton wire consisted of the chromophore and the newly inserted Asp-148 at a very short hydrogen-bond distance of 2.4 Å.[56,57] This mutant shows a (distorted) neutral-like chromophore absorption and anionic-like emission. The precise protonation states of absorbing and fluorescent states in this mutant were not

dx.doi.org/10.1021/jp401114e | J. Phys. Chem. B XXXX, XXX, XXX−XXX

entirely clear-cut: femtosecond fluorescence and transient absorption experiments failed to resolve a rise of the anionic emission.[57−59] In addition, no dynamic protonation of the Asp-148 carboxyl side chain was observed with ultrafast mid-IR spectroscopy,[60] which contrasts to the situation in wild-type GFP where clear protonation of the initial anionic Glu-222 side chain on a ps time scale was reported.[27,31,32] Thus, apparently Asp-148 does not become protonated in the S65T/H148D GFP mutant upon excitation. These seemingly contradictory observations of on one hand neutral absorption and anionic emission spectra and on the other hand kinetically unresolved proton transfer processes could be explained with the existence of a low-barrier hydrogen bond (LBHB)[61,62] between the chromophore and Asp-148, which implies a delocalization of a proton between donor and acceptor, in a shared polar covalent bond with both oxygens.[60]

Our observations in psamFP488 are fundamentally different from those in the GFP S65T/H148D mutant. In this work, we clearly resolve a rise of the stimulated emission from the anionic chromophore I* in 170 fs. In addition, we resolve the short-lived (110 fs) absorption of the dumped anionic ground state I, evidencing ultrafast, discrete proton shuttling events in psamFP488 in both directions. We conclude that, in all observed intermediates shown in Figures 5 and 6, the proton is localized either on the chromophore (in A and A*) or on Glu-167 (in I and I*). Hence, although the hydrogen-bond geometry between the chromophore and Glu-167 facilitates ultrafast proton shuttling, possibly through a short hydrogen bond, we conclude that it does not correspond to a low-barrier hydrogen bond. From a structural viewpoint, this is not unexpected, given that the proton acceptor groups in psamFP488 and the S65T/H148D GFP mutant are in different positions with respect to the chromophore phenol group.

CONCLUSIONS

PsamFP488 demonstrates a novel mechanism of cyan color generation that involves a glutamic acid residue in position 167. This position has been shown to exhibit strong statistical correlation with the biological evolution of cyan color from a common green ancestor.[40] However, ESPT has not previously been observed to be the underlying mechanism of cyan fluorescence in any GFP-like protein. Here, we demonstrate that ESPT lies at the basis of a large Stokes shift in psamFP488. The ESPT reaction is unusually fast and occurs with a time constant of 170 fs, as evidenced by the rise of the stimulated emission of the anionic chromophore. Upon dumping the excited state with an ultrafast laser pulse, we clearly observe the ground-state absorption of the anionic chromophore with an absorption maximum at 484 nm. Remarkably, this ground-state species disappears very rapidly with a time constant of 110 fs, which indicates that the proton is shuttled back to the chromophore in the ground state as fast as the chromophore deprotonates in the excited state. To the best of our knowledge, this result represents the fastest experimentally observed proton transfer process in a molecular ground state.

The very fast, discrete proton transfer reactions in psamFP488 imply that the local structure around the chromophore is preconfigured, involving a favorable hydrogen-bond geometry without the need for structural relaxation prior to proton transfer, possibly facilitated by a short hydrogen bond between chromophore and Glu-167. In contrast to the situation in the S65T/H148D mutant of GFP,[56,57,59,60] most likely no low-barrier hydrogen bond exists between chromophore and proton acceptor group. This work supports the notion that proton transfer, be it in an electronic excited or ground state, can be an intrinsically fast process that occurs on a 100 fs time scale. Thus, psamFP488 represents an attractive model system that poses an ultrafast proton transfer regime in discrete steps. It constitutes a valuable model system in addition to wild type GFP, where proton transfer is relatively slow, and the S65T/H148D GFP mutant, where the effects of low-barrier hydrogen bonds dominate. Unfortunately, we do not have detailed structural information on this highly interesting biological proton transfer system: efforts are underway to determine the X-ray structure of psamFP488.

ASSOCIATED CONTENT

Supporting Information

Figures showing kinetics at selected wavelengths, elaborate target analysis results, and photoconversion in psam488. This material is available free of charge via the Internet at http://pubs.acs.org.

AUTHOR INFORMATION

Corresponding Author

*E-mail: j.t.m.kennis@vu.nl (J.T.M.K.); Rebekka.Wachter@asu.edu (R.M.W.).

Notes

The authors declare no competing financial interest.

ACKNOWLEDGMENTS

J.T.M.K was supported by The Netherlands Organization for Scientific Research, Chemical Sciences Council (NWO-CW), through a VICI grant. Further, this work was supported by the National Science Foundation (NSF) Grant No. MCB-0615938 to R.M.W. A.P. was supported by HARVEST Marie Curie Research Training Network (PITN-GA-2009-238017). This work was supported by a NWO-CW equipment investment grant to J.T.M.K.

ABBREVIATIONS

ESPT, excited-state proton transfer; CFP, cyan fluorescent protein; FRET, Förster resonance energy transfer; EADS, evolution-associated difference spectrum; SADS, species-associated difference spectrum; LBHB, low-barrier hydrogen bond

REFERENCES

(1) Alieva, N. O.; Konzen, K. A.; Field, S. F.; Meleshkevitch, E. A.; Hunt, M. E.; Beltran-Ramirez, V.; Miller, D. J.; Wiedenmann, J.; Salih, A.; Matz, M. V. Diversity and Evolution of Coral Fluorescent Proteins. *PLoS One* **2008**, 3.

(2) Chudakov, D. M.; Matz, M. V.; Lukyanov, S.; Lukyanov, K. A. Fluorescent Proteins and Their Applications in Imaging Living Cells and Tissues. *Physiol. Rev.* **2010**, *90*, 1103−1163.

(3) Tsien, R. Y. The Green Fluorescent Protein. *Annu. Rev. Biochem.* **1998**, *67*, 509−544.

(4) Markwardt, M. L.; Kremers, G.-J.; Kraft, C. A.; Ray, K.; Cranfill, P. J. C.; Wilson, K. A.; Day, R. N.; Wachter, R. M.; Davidson, M. W.; Rizzo, M. A. In Improved Cerulean Fluorescent Protein with Enhanced Brightness and Reduced Reversible Photoswitching. *PLoS One* **2011**, *6*, e17896.

(5) Watkins, J. L.; Kim, H.; Markwardt, M. L.; Chen, L.; Fromme, R.; Rizzo, M. A.; Wachter, R. M. The 1.6 Å Resolution Structure of a FRET-optimized Cerulean Fluorescent Protein. *Acta Crystallogr., Sect. D* **2013**, DOI: 10.1107/S0907444913001546.

(6) Goedhart, J.; von Stetten, D.; Noirclerc-Savoye, M.; Lelimousin, M.; Joosen, L.; Hink, M. A.; van Weeren, L.; Gadella, T. W. J.; Royant, A. Structure-Guided Evolution of Cyan Fluorescent Proteins Towards a Quantum Yield of 93%. *Nat. Commun.* **2012**, *3*, 1738/1−1738/9.
(7) Kogure, T.; Kawano, H.; Abe, Y.; Miyawaki, A. Fluorescence Imaging Using a Fluorescent Protein with a Large Stokes Shift. *Methods* **2008**, *45*, 223−226.
(8) Ai, H. W.; Henderson, J. N.; Remington, S. J.; Campbell, R. E. Directed Evolution of a Monomeric, Bright and Photostable Version of Clavularia Cyan Fluorescent Protein: Structural Characterization and Applications in Fluorescence Imaging. *Biochem. J.* **2006**, *400*, 531−540.
(9) Carlson, H. J.; Campbell, R. E. Genetically Encoded FRET-Based Biosensors for Multiparameter Fluorescence Imaging. *Curr. Opin. Biotechnol.* **2009**, *20*, 19−27.
(10) Chattoraj, M.; King, B. A.; Bublitz, G. U.; Boxer, S. G. Ultra-Fast Excited State Dynamics in Green Fluorescent Protein: Multiple States and Proton Transfer. *Proc. Natl. Acad. Sci. U.S.A.* **1996**, *93*, 8362−8367.
(11) Winkler, K.; Lindner, J. R.; Subramaniam, V.; Jovin, T. M.; Vohringer, P. Ultrafast Dynamics in the Excited State of Green Fluorescent Protein (wt) Studied by Frequency-Resolved Femtosecond Pump-Probe Spectroscopy. *Phys. Chem. Chem. Phys.* **2002**, *4*, 1072−1081.
(12) Kennis, J. T. M.; Larsen, D. S.; van Stokkum, I. H. M.; Vengris, M.; van Thor, J. J.; van Grondelle, R. Uncovering the Hidden Ground State of Green Fluorescent Protein. *Proc. Natl. Acad. Sci. U.S.A.* **2004**, *101*, 17988−17993.
(13) Creemers, T. M. H.; Lock, A. J.; Subramaniam, V.; Jovin, T. M.; Volker, S. Three Photoconvertible Forms of Green Fluorescent Protein Identified by Spectral Hole-Burning. *Nat. Struct. Biol.* **1999**, *6*, 557−560.
(14) Brejc, K.; Sixma, T. K.; Kitts, P. A.; Kain, S. R.; Tsien, R. Y.; Ormo, M.; Remington, S. J. Structural Basis for Dual Excitation and Photoisomerization of the Aequorea victoria Green Fluorescent Protein. *Proc. Natl. Acad. Sci. U.S.A.* **1997**, *94*, 2306−2311.
(15) Toh, K. C.; Stojkovic, E. A.; van Stokkum, I. H. M.; Moffat, K.; Kennis, J. T. M. Proton-Transfer and Hydrogen-Bond Interactions Determine Fluorescence Quantum Yield and Photochemical Efficiency of Bacteriophytochrome. *Proc. Natl. Acad. Sci. U.S.A.* **2010**, *107*, 9170−9175.
(16) Toh, K. C.; Stojkovic, E. A.; van Stokkum, I. H. M.; Moffat, K.; Kennis, J. T. M. Fluorescence Quantum Yield and Photochemistry of Bacteriophytochrome Constructs. *Phys. Chem. Chem. Phys.* **2011**, *13*, 11985−11997.
(17) Carroll, E. C.; Song, S.-H.; Kumauchi, M.; van Stokkum, I. H. M.; Jailaubekov, A.; Hoff, W. D.; Larsen, D. S. Subpicosecond Excited-State Proton Transfer Preceding Isomerization during the Photorecovery of Photoactive Yellow Protein. *J. Phys. Chem. Lett.* **2010**, *1*, 2793−2799.
(18) Kennis, J. T. M.; Crosson, S.; Gauden, M.; van Stokkum, I. H. M.; Moffat, K.; van Grondelle, R. Primary Reactions of the LOV2 Domain of Phototropin, a Plant Blue-Light Photoreceptor. *Biochemistry* **2003**, *42*, 3385−3392.
(19) Mathes, T.; van Stokkum, I. H. M.; Stierl, M.; Kennis, J. T. M. Redox Modulation of Flavin and Tyrosine Determines Photoinduced Proton-Coupled Electron Transfer and Photoactivation of BLUF Photoreceptors. *J. Biol. Chem.* **2012**, *287*, 31725−31738.
(20) Toh, K. C.; van Stokkum, I. H. M.; Hendriks, J.; Alexandre, M. T. A.; Arents, J. C.; Perez, M. A.; van Grondelle, R.; Hellingwerf, K. J.; Kennis, J. T. M. On the Signaling Mechanism and the Absence of Photoreversibility in the AppA BLUF Domain. *Biophys. J.* **2008**, *95*, 312−321.
(21) Gauden, M.; van Stokkum, I. H. M.; Key, J. M.; Luehrs, D. C.; Van Grondelle, R.; Hegemann, P.; Kennis, J. T. M. Hydrogen-Bond Switching through a Radical Pair Mechanism in a Flavin-Binding Photoreceptor. *Proc. Natl. Acad. Sci. U.S.A.* **2006**, *103*, 10895−10900.
(22) Bonetti, C.; Mathes, T.; van Stokkum, I. H. M.; Mullen, K. M.; Groot, M.-L.; van Grondelle, R.; Hegemann, P.; Kennis, J. T. M. Hydrogen Bond Switching among Flavin and Amino Acid Side Chains in the BLUF Photoreceptor Observed by Ultrafast Infrared Spectroscopy. *Biophys. J.* **2008**, *95*, 4790−4802.
(23) Kennis, J. T. M.; Groot, M.-L. Ultrafast Spectroscopy of Biological Photoreceptors. *Curr. Opin. Struct. Biol.* **2007**, *17*, 623−630.
(24) Immeln, D.; Weigel, A.; Kottke, T.; Perez Lustres, J. L. Primary Events in the Blue Light Sensor Plant Cryptochrome: Intraprotein Electron and Proton Transfer Revealed by Femtosecond Spectroscopy. *J. Am. Chem. Soc.* **2012**, *134*, 12536−12546.
(25) Mathes, T.; van Stokkum, I. H. M.; Bonetti, C.; Hegemann, P.; Kennis, J. T. M. The Hydrogen-Bond Switch Reaction of the Blrb Bluf Domain of Rhodobacter sphaeroides. *J. Phys. Chem. B* **2011**, *115*, 7963−7971.
(26) Gauden, M.; Grinstead, J. S.; Laan, W.; van Stokkum, I. H. M.; Avila-Perez, M.; Toh, K. C.; Boelens, R.; Kaptein, R.; van Grondelle, R.; Hellingwerf, K. J.; Kennis, J. T. M. On the Role of Aromatic Side Chains in the Photoactivation of BLUF Domains. *Biochemistry* **2007**, *46*, 7405−7415.
(27) Stoner-Ma, D.; Jaye, A. A.; Matousek, P.; Towrie, M.; Meech, S. R.; Tonge, P. J. Observation of Excited-State Proton Transfer in Green Fluorescent Protein Using Ultrafast Vibrational Spectroscopy. *J. Am. Chem. Soc.* **2005**, *127*, 2864−2865.
(28) van Stokkum, I. H. M.; Gobets, B.; Gensch, T.; van Mourik, F.; Hellingwerf, K. J.; van Grondelle, R.; Kennis, J. T. M. (Sub)-Picosecond Spectral Evolution of Fluorescence in Photoactive Proteins Studied with a Synchroscan Streak Camera System. *Photochem. Photobiol.* **2006**, *82*, 380−388.
(29) Jaye, A. A.; Stoner-Ma, D.; Matousek, P.; Towrie, M.; Tonge, P. J.; Meech, S. R. Time-Resolved Emission Spectra of Green Fluorescent Protein. *Photochem. Photobiol.* **2006**, *82*, 373−379.
(30) van Thor, J. J.; Ronayne, K. L.; Towrie, M.; Sage, J. T. Balance between Ultrafast Parallel Reactions in the Green Fluorescent Protein Has a Structural Origin. *Biophys. J.* **2008**, *95*, 1902−1912.
(31) Di Donato, M.; van Wilderen, L. J. G. W.; Van Stokkum, I. H. M.; Stuart, T. C.; Kennis, J. T. M.; Hellingwerf, K. J.; van Grondelle, R.; Groot, M. L. Proton Transfer Events in GFP. *Phys. Chem. Chem. Phys.* **2011**, *13*, 16295−16305.
(32) van Thor, J. J.; Zanetti, G.; Ronayne, K. L.; Towrie, M. Structural Events in the Photocycle of Green Fluorescent Protein. *J. Phys. Chem. B* **2005**, *109*, 16099−16108.
(33) Malo, G. D.; Wang, M.; Wu, D.; Stelling, A. L.; Tonge, P. J.; Wachter, R. M. Crystal Structure and Raman Studies of dsFP483, a Cyan Fluorescent Protein from Discosoma striata. *J. Mol. Biol.* **2008**, *378*, 869−884.
(34) Berera, R.; van Grondelle, R.; Kennis, J. T. M. Ultrafast Transient Absorption Spectroscopy: Principles and Application to Photosynthetic Systems. *Photosynth. Res.* **2009**, *101*, 105−118.
(35) Bonetti, C.; Stierl, M.; Mathes, T.; van Stokkum, I. H. M.; Mullen, K. M.; Cohen-Stuart, T. A.; van Grondelle, R.; Hegemann, P.; Kennis, J. T. M. The Role of Key Amino Acids in the Photoactivation Pathway of the Synechocystis Slr1694 BLUF Domain. *Biochemistry* **2009**, *48*, 11458−11469.
(36) van Oort, B.; ter Veer, M. J. T.; Groot, M. L.; van Stokkum, I. H. M. Excited State Proton Transfer in Strongly Enhanced GFP (sGFP2). *Phys. Chem. Chem. Phys.* **2012**, *14*, 8852−8858.
(37) Remington, S. J.; Wachter, R. M.; Yarbrough, D. K.; Branchaud, B.; Anderson, D. C.; Kallio, K.; Lukyanov, K. A. zFP538, a Yellow-Fluorescent Protein from Zoanthus, Contains a Novel Three-Ring Chromophore. *Biochemistry* **2005**, *44*, 202−212.
(38) Pletneva, N.; Pletnev, V.; Tikhonova, T.; Pakhomov, A. A.; Popov, V.; Martynov, V. I.; Wlodawer, A.; Dauter, Z.; Pletnev, S. Refined Crystal Structures of Red and Green Fluorescent Proteins from the Button Polyp Zoanthus. *Acta Crystallogr., Sect. D* **2007**, *63*, 1082−1093.
(39) Henderson, J. N.; Remington, S. J. Crystal Structures and Mutational Analysis of amFP486, a Cyan Fluorescent Protein from Anemonia majano. *Proc. Natl. Acad. Sci. U.S.A.* **2005**, *102*, 12712−12717.

(40) Field, S. F.; Bulina, M. Y.; Kelmanson, I. V.; Bielawski, J. P.; Matz, M. V. Adaptive Evolution of Multicolored Fluorescent Proteins in Reef-Building Corals. *J. Mol. Evol.* **2006**, *62*, 332−339.
(41) van Thor, J. J.; Gensch, T.; Hellingwerf, K. J.; Johnson, L. N. Phototransformation of Green Fluorescent Protein with UV and Visible Light Leads to Decarboxylation of Glutamate 222. *Nat. Struct. Biol.* **2002**, *9*, 37−41.
(42) Gai, F.; McDonald, J. C.; Anfinrud, P. A. Pump-Dump-Probe Spectroscopy of Bacteriorhodosin: Evidence for a near-IR Excited State Absorbance. *J. Am. Chem. Soc.* **1997**, *119*, 6201−6202.
(43) Ruhman, S.; Hou, B. X.; Friedman, N.; Ottolenghi, M.; Sheves, M. Following Evolution of Bacteriorhodopsin in Its Reactive Excited State via Stimulated Emission Pumping. *J. Am. Chem. Soc.* **2002**, *124*, 8854−8858.
(44) Larsen, D. S.; van Stokkum, I. H. M.; Vengris, M.; van der Horst, M. A.; de Weerd, F. L.; Hellingwerf, K. J.; van Grondelle, R. Incoherent Manipulation of the Photoactive Yellow Protein Photocycle with Dispersed Pump-Dump-Probe Spectroscopy. *Biophys. J.* **2004**, *87*, 1858−1872.
(45) Kim, P. W.; Freer, L. H.; Rockwell, N. C.; Martin, S. S.; Lagarias, J. C.; Larsen, D. S. Second-Chance Forward Isomerization Dynamics of the Red/Green Cyanobacteriochrome NpR6012g4 from Nostoc punctiforme. *J. Am. Chem. Soc.* **2012**, *134*, 130−133.
(46) Papagiannakis, E.; Vengris, M.; Larsen, D. S.; van Stokkum, I. H. M.; Hiller, R. G.; van Grondelle, R. Use of Ultrafast Dispersed Pump-Dump-Probe and Pump-Repump-Probe Spectroscopies to Explore the Light-Induced Dynamics of Peridinin in Solution. *J. Phys. Chem. B* **2006**, *110*, 512−521.
(47) Papagiannakis, E.; Larsen, D. S.; van Stokkum, I. H. M.; Vengris, M.; Hiller, R. G.; van Grondelle, R. Resolving the Excited State Equilibrium of Peridinin in Solution. *Biochemistry* **2004**, *43*, 15303−15309.
(48) Rupenyan, A.; van Stokkum, I. H. M.; Arents, J. C.; van Grondelle, R.; Hellingwerf, K. J.; Groot, M. L. Reaction Pathways of Photoexcited Retinal in Proteorhodopsin Studied by Pump-Dump-Probe Spectroscopy. *J. Phys. Chem. B* **2009**, *113*, 16251−16256.
(49) Vengris, M.; Larsen, D. S.; van der Horst, M. A.; Larsen, O. F. A.; Hellingwerf, K. J.; van Grondelle, R. Ultrafast Dynamics of Isolated Model Photoactive Yellow Protein Chromophores: "Chemical Perturbation Theory" in the Laboratory. *J. Phys. Chem. B* **2005**, *109*, 4197−4208.
(50) Vengris, M.; van Stokkum, I. H. M.; He, X.; Bell, A. F.; Tonge, P. J.; van Grondelle, R.; Larsen, D. S. Ultrafast Excited and Ground-State Dynamics of the Green Fluorescent Protein Chromophore in Solution. *J. Phys. Chem. A* **2004**, *108*, 4587−4598.
(51) Mathes, T.; Zhu, J.; van Stokkum, I. H. M.; Groot, M. L.; Hegemann, P.; Kennis, J. T. M. Hydrogen Bond Switching among Flavin and Amino Acids Determines the Nature of Proton-Coupled Electron Transfer in BLUF Photoreceptors. *J. Phys. Chem. Lett.* **2012**, *3*, 203−208.
(52) Zhu, J.; Paparelli, L.; Hospes, M.; Arents, J. C.; Kennis, J. T. M.; van Stokkum, I. H. M.; Hellingwerf, K. J.; Groot, M. L. Photoionization and Electron Radical Recombination Dynamics in Photoactive Yellow Protein Investigated by Ultrafast Spectroscopy in the Visible and Near-Infrared Spectral Region. *J. Phys. Chem. B* **2013**, DOI: 10.1021/jp311906f.
(53) Kuznetsov, A. M.; Ulstrup, J. Proton and Hydrogen Atom Tunnelling in Hydrolytic and Redox Enzyme Catalysis. *Can. J. Chem.* **1999**, *77*, 1085−1096.
(54) Herek, J. L.; Pedersen, S.; Banares, L.; Zewail, A. H. Femtosecond Real-Time Probing of Reactions. 9. Hydrogen-Atom Transfer. *J. Chem. Phys.* **1992**, *97*, 9046−9061.
(55) Fang, C.; Frontiera, R. R.; Tran, R.; Mathies, R. A. Mapping GFP Structure Evolution during Proton Transfer with Femtosecond Raman Spectroscopy. *Nature* **2009**, *462*, 200−U74.
(56) Shu, X.; Kallio, K.; Shi, X.; Abbyad, P.; Kanchanawong, P.; Childs, W.; Boxer, S. G.; Remington, S. J. Ultrafast Excited-State Dynamics in the Green Fluorescent Protein Variant S65T/H148D. 1. Mutagenesis and Structural Studies. *Biochemistry* **2007**, *46*, 12005−12013.
(57) Shi, X.; Abbyad, P.; Shu, X.; Kallio, K.; Kanchanawong, P.; Childs, W.; Remington, S. J.; Boxer, S. G. Ultrafast Excited-State Dynamics in the Green Fluorescent Protein Variant S65T/H148D. 2. Unusual Photophysical Properties. *Biochemistry* **2007**, *46*, 12014−12025.
(58) Leiderman, P.; Genosar, L.; Huppert, D.; Shu, X.; Remington, S. J.; Solntsev, K. M.; Tolbert, L. M. Ultrafast Excited-State Dynamics in the Green Fluorescent Protein Variant S65T/H148D. 3. Short- and Long-Time Dynamics of the Excited-State Proton Transfer. *Biochemistry* **2007**, *46*, 12026−12036.
(59) Kondo, M.; Heisler, I. A.; Stoner-Ma, D.; Tonge, P. J.; Meech, S. R. Ultrafast Dynamics of Protein Proton Transfer on Short Hydrogen Bond Potential Energy Surfaces: S65T/H148D GFP. *J. Am. Chem. Soc.* **2010**, *132*, 1452−+.
(60) Stoner-Ma, D.; Jaye, A. A.; Ronayne, K. L.; Nappa, J.; Meech, S. R.; Tonge, P. J. An Alternate Proton Acceptor for Excited-State Proton Transfer in Green Fluorescent Protein: Rewiring GFP. *J. Am. Chem. Soc.* **2008**, *130*, 1227−1235.
(61) Cleland, W. W.; Kreevoy, M. M. Low-Barrier Hydrogen-Bonds and Enzymatic Catalysis. *Science* **1994**, *264*, 1887−1890.
(62) Schiott, B.; Iversen, B. B.; Madsen, G. K. H.; Larsen, F. K.; Bruice, T. C. On the Electronic Nature of Low-Barrier Hydrogen Bonds in Enzymatic Reactions. *Proc. Natl. Acad. Sci. U.S.A.* **1998**, *95*, 12799−12802.